

Electronic Supplementary Information

**Pristine, Metal Ion and Metal Cluster Modified
Conjugated Triazine Frameworks as
Electrocatalysts for Hydrogen Evolution
Reaction**

Boying Zhang,^a Yunrui Zhang,^{a,c} Meiling Hou,^{*,b} Wenbo Wang,^c Shuozhen
Hu,^c Wanglai Cen,^d Xuepu Cao,^a Shanlin Qiao,^{*,a} Bao-Hang Han^{*,e,f}

^a *College of Chemistry and Pharmaceutical Engineering, Hebei University
of Science and Technology, Shijiazhuang 050018, China*

^b *College of Engineering, Hebei Normal University, Shijiazhuang 050024,
China*

^c *State Key Laboratory of Chemical Engineering, East China University of
Science and Technology, Shanghai 200237, China*

^d *Institute of New Energy and Low Carbon Technology and the National
Engineering, Sichuan University, Chengdu 610065, China*

^e *CAS Key Laboratory of Nanosystem and Hierarchical Fabrication, CAS
Center for Excellence in Nanoscience, National Center for Nanoscience
and Technology, Beijing 100190, China*

^f *University of Chinese Academy of Sciences, Beijing 100049, China*

Experimental Section

Materials

Pyridine-2,6-dicarbonitrile, ZnCl_2 , $\text{Pd}(\text{NO}_3)_2$, K_2PtCl_4 , H_2PtCl_6 , and $\text{Pd}(\text{OAc})_2$ reagents were purchased from Aladdin. 5,5'-Dicyano-2,2'-bipyridine was purchased from Zhengzhou Alfa Chemical Co. Ltd. $\text{CuCl}_2 \cdot 2\text{H}_2\text{O}$, $\text{CoCl}_2 \cdot 6\text{H}_2\text{O}$, $\text{NiCl}_2 \cdot 6\text{H}_2\text{O}$, ethanol, tetrahydrofuran (THF), and acetone was purchased from Tianjin Damao Chemical Co. Ltd. All chemicals are of reagent grade and used directly without further purification.

Preparation

Synthesis of BPY-CTF: The BPY-CTF was prepared according to previous literature.^{S1} 5,5'-Dicyano-2,2'-bipyridine (BPY, 160.8 mg, 0.78 mmol) and zinc chloride (ZnCl_2 , 531.2 mg, 3.9 mmol) were placed into Pyrex tube under the protection of nitrogen atmosphere. The Pyrex tube was evacuated, sealed, and heated to 600 °C for 48 h, with the heating rate of 1 °C min^{-1} . The product was collected after the reaction system cooled to room temperature. The black powder was treated with deionized water and dilute hydrochloric acid (1 mol L^{-1}). Then, the obtained black powder was dripped washing in turn with deionized water (3×10 mL), THF (3×10 mL), and acetone (3×10 mL). Finally, the product was dried in vacuum at 100 °C for 24 h.

Synthesis of DCP-CTF: The synthetic procedure of DCP-CTF is similar to BPY-CTF. Pyridine-2,6-dicarbonitrile (DCP, 127.8 mg, 0.99 mmol) and zinc chloride (ZnCl_2 ,

667.4 mg, 4.9 mmol) were put into Pyrex tube under the protection of nitrogen atmosphere. The Pyrex tube was evacuated, sealed, and heated to 400 °C for 10 h and then heated 600 °C for 10 h. The heating rate is 5 °C min⁻¹. The Pyrex tube was opened when it was cooled to room temperature. The black powder was treated with deionized water and dilute hydrochloric acid (1 mol L⁻¹). Then, the filtered black powder was washed in turn with deionized water (3×10 mL), THF (3×10 mL), and acetone (3×10 mL). Finally, the product was dried in vacuum at 100 °C for 24 h.

Synthesis of CTF-M²⁺: The as-synthesized BPY-CTF (20 mg) was separately treated with CuCl₂·2H₂O (14.6 mg, 0.096 mmol), CoCl₂·6H₂O (22.8 mg, 0.096 mmol), NiCl₂·6H₂O (22.8 mg, 0.096 mmol), Pd(NO₃)₂ (22.1 mg, 0.096 mmol), and K₂PtCl₄ (39.8 mg, 0.096 mmol) in deionized water (25 mL). The solution containing Co²⁺, Ni²⁺, or Cu²⁺ was heated to 60 °C for 4 h under stirring. Analogously, the solution containing Pt²⁺ or Pd²⁺ was stirred for 3 h at 80 °C, following which it was washed with deionized water (3×10 mL) and ethyl alcohol (3×10 mL). Thus, the obtained materials (named as BPY-CTF-Cu²⁺, BPY-CTF-Co²⁺, BPY-CTF-Ni²⁺, BPY-CTF-Pd²⁺, and BPY-CTF-Pt²⁺) were dried using vacuum for 24 h at 60 °C.

The as-prepared DCP-CTF (20 mg) was treated with CuCl₂·2H₂O (35.1 mg, 0.23 mmol), CoCl₂·6H₂O (54.7 mg, 0.23 mmol), NiCl₂·6H₂O (54.7 mg, 0.23 mmol), Pd(NO₃)₂ (53.0 mg, 0.23 mmol), and K₂PtCl₄ (95.5 mg, 0.23 mmol) in 25 mL deionized water (25 mL). The solution containing Co²⁺, Ni²⁺, or Cu²⁺ was heated to 60 °C for 4 h under stirring. Analogously, the solution containing Pt²⁺ or Pd²⁺ was stirred for 3 h at 80

°C. The raw product was washed with deionized water (3×10 mL) and ethyl alcohol (3×10 mL). Thus, the obtained materials (named as DCP-CTF-Cu²⁺, DCP-CTF-Co²⁺, DCP-CTF-Ni²⁺, DCP-CTF-Pd²⁺, and DCP-CTF-Pt²⁺) were dried under vacuum for 24 h at 60 °C.

Synthesis of BPY-CTF@Pt-MC: The BPY-CTF (50 mg) was dispersed in ultra-pure water (20 mL) and the mixture was treated with ultrasonic for 0.5 h to form evenly distributed suspension. Then, the suspension was added to a 10 mL deionized water solution containing H₂PtCl₆·6H₂O (10 mg, 0.019 mmol). Then, NaBH₄ (8.25 g, 0.218 mol) was dissolved in deionized water (15 mL) and the mixture was added to the above-mentioned mixed solution by dropping under stirring for 2 h. The final mixture solution stayed overnight. Subsequently, the product was collected by filtration and washed with deionized water (3×4 mL) and ethanol (3×4 mL). The product named BPY-CTF@Pt-MC was dried under vacuum at 60 °C overnight.

Synthesis of BPY-CTF@Pd-MC: The palladium acetate powder (13 mg, 0.058 mmol) was dissolved in dichloromethane (15 mL) and the solution was stirred for 30 min, then the BPY-CTF (90 mg) was added in the solution. After that the mixture was stirred for 24 h at room temperature. The obtained solid was centrifuged and extracted with dichloromethane soxhlet for 24 h. Then, BPY-CTF@Pd-MC was dried under vacuum at 80 °C overnight.

Synthesis of BPY-CTF@Cu-MC, BPY-CTF@Co-MC, and BPY-CTF@Ni-MC: CuCl₂·2H₂O (2.546 g, 16.7 mmol), CoCl₂·6H₂O (3.973 g, 16.7 mmol), or

NiCl₂·6H₂O (3.969 mg, 16.7 mmol), sodium dodecylsulfate (SDS, 1.442 mg, 5 mmol), and BPY-CTF (60 mg) was dissolved in ultra-pure water (10 mL) with stirring for 3 h, respectively. Then, aqueous NaOH solution (1 M, 3.5 mL) was added under stirring for 30 min. Finally, aqueous NaH₂PO₂ solution (0.34 M, 5 mL) was added to the above solution and the mixture solution was stirred continuously for 30 min to get a uniform solution. The solution was transferred into Teflon-lined autoclave, which was heated at 110 °C for 48 h, and 100 °C for 12 h. Then, the solution was treated and centrifuged with water and ethanol for five times, respectively. The products were dried under vacuum at 60 °C (named as BPY-CTF@Ni-MC, BPY-CTF@Co-MC, and BPY-CTF@Cu-MC).

Synthesis of DCP-CTF@M: The synthetic procedure of DCP-CTF@Cu-MC, DCP-CTF@Co-MC, DCP-CTF@Ni-MC, DCP-CTF@Pd-MC, and DCP-CTF@Pt-MC were same as the counterpart BPY-CTF@Cu-MC, BPY-CTF@Co-MC, BPY-CTF@Ni-MC, BPY-CTF@Pd-MC, and BPY-CTF@Pt-MC except for that BPY-CTF was changed to DCP-CTF.

Instrumental characterization

The crystal structures of the samples were characterized using X-ray diffractometer (XRD, X' Pert PRO, Cu K α , λ = 0.1542 nm). Fourier transform infrared (FT-IR) spectra of the samples were obtained with a Thermo Scientific Nicolet iS10 spectrometer. The morphologies of the samples were recorded by a JEOL scanning electron microscope (SEM) equipped with an energy-dispersive spectrometer. The

STEM images were acquired on spherical aberration correction field emission transmission electron microscope (FEI Theims Z). TEM and HRTEM images were obtained on a transmission electron microscope (JEOL, JEM-2100). Nitrogen sorption measurements were conducted with a Quantachrome Autosorb apparatus at 77 K. The specific surface areas were calculated by the Brunauer–Emmett–Teller (BET) method. The samples were degassed at 150 °C for 12 h before measurements. The Raman spectra were measured by Raman Spectrometer (HORIBA Scientific LabRAM HR Evolution). The XPS data were collected on Thermo Scientific K-Alpha spectrometer.

Electrochemical measurements of all samples were performed using an electrochemical workstation (Princeton) with three-electrode system. The three-electrode setup was composed of working, counter, and reference electrodes, which were a glass carbon electrode (4 mm in diameter) coated with catalyst, a platinum plate, and Ag/AgCl (sat. KCl), respectively. The electrocatalytic performances of the CTFs-based electrocatalysts were tested in N₂-saturated aqueous H₂SO₄ solution (0.5 mol L⁻¹). All the potentials were converted with respect to RHE using the following formula:

$$E_{RHE} = E_{Ag/AgCl} + 0.197 V + 0.0591 \times pH$$

The scan rate of linear sweep voltammetry (LSV) was 5 mV s⁻¹. Electrochemical impedance spectroscopy (EIS) were measured with a frequency from 100 kHz to 100 mHz and an AC voltage of 5 mV. The double layer capacitance (C_{dl}) was obtained by cyclic voltammetry (CV) under the potential windows from 0.00–0.20 V vs. RHE with different scan rate of 20, 40, 60, 80 and 100 mV s⁻¹. The differences in current density

variation ($\Delta J = J_a - J_c$, where J_a and J_c are the anodic and cathodic current, respectively) at an overpotential of 0.10 V plotted against scan rate fitted to a linear regression enables the estimation of C_{dl} for CTFs-based electrocatalysts.

The catalyst ink solutions were prepared by adding 4 mg of each catalyst and 30 μL of 5 wt % Nafion in 1 mL of water/ethanol (V/V=3:1) mixture solution. The mixed suspensions were ultrasonicated for 1 h. Then, 5 μL of each catalyst ink was uniformly dispersed on the polished glass carbon electrode and dried at room temperature. The catalyst loading on glass carbon electrode was about 0.159 mg cm^{-2} .

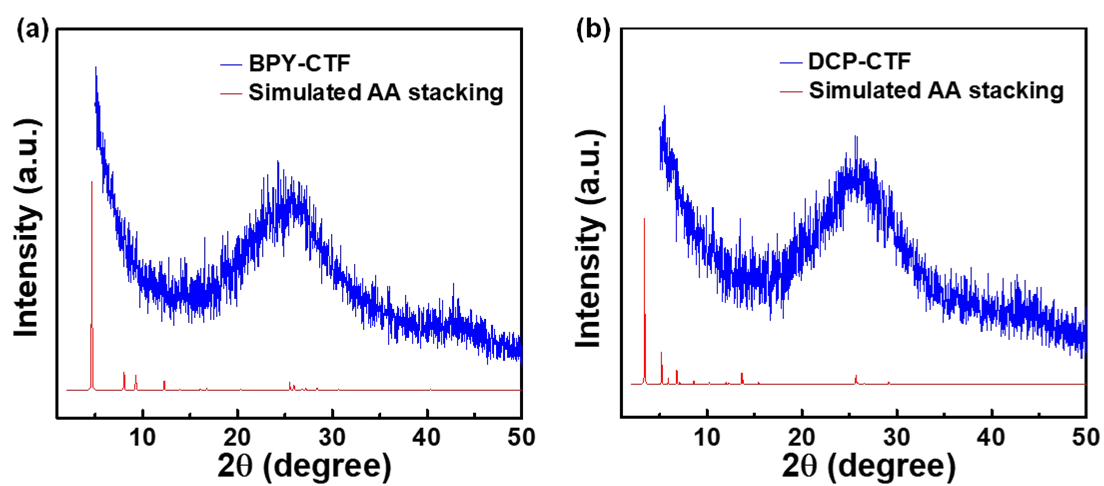


Fig. S1 P-XRD pattern of experimental and simulated AA stacking of (a) DCP-CTF and (b) BPY-CTF.

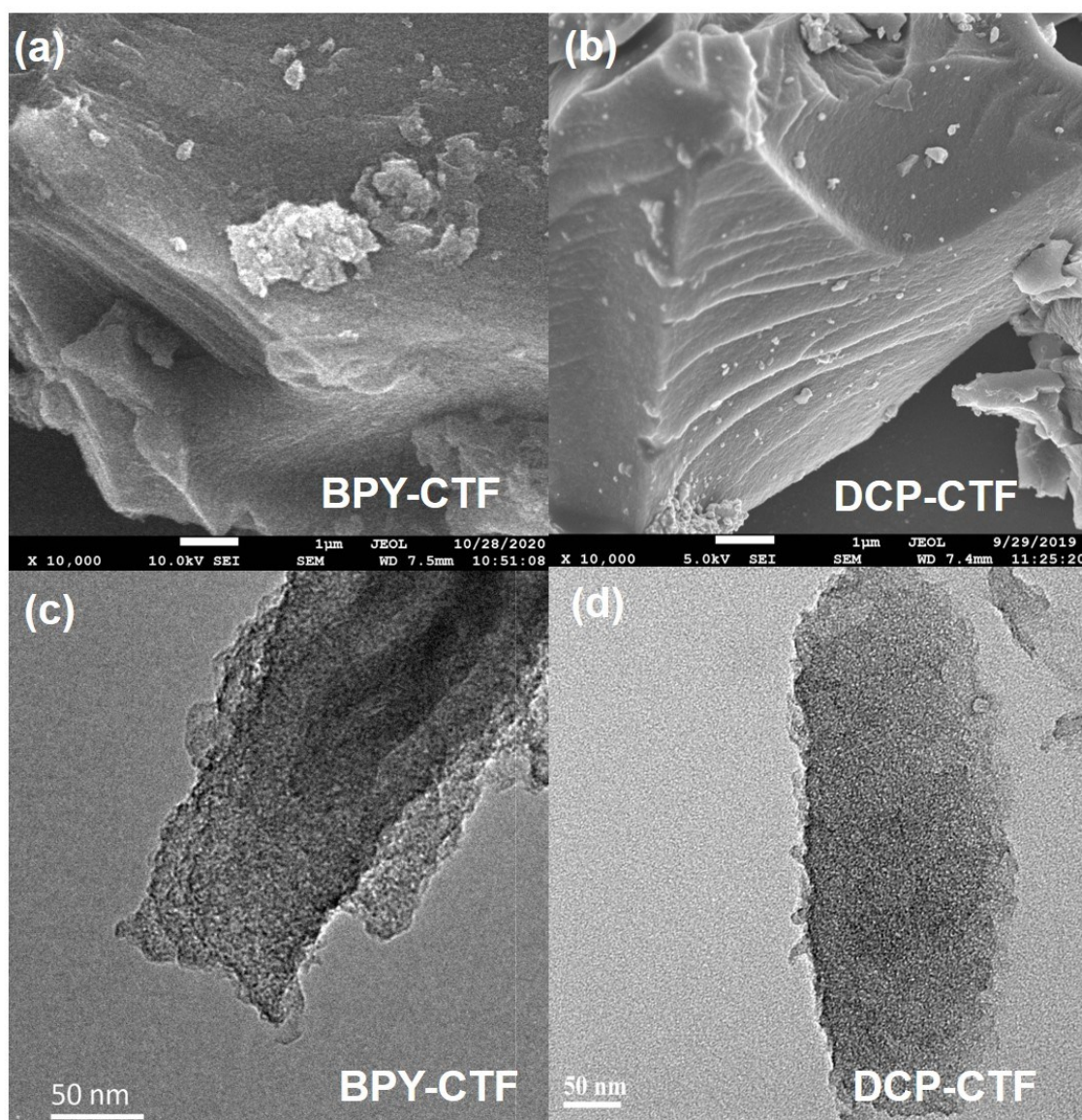


Fig. S2 The SEM images of (a) BPY-CTF and (b) DCP-CTF. The TEM images of (c) BPY-CTF and (d) DCP-CTF.

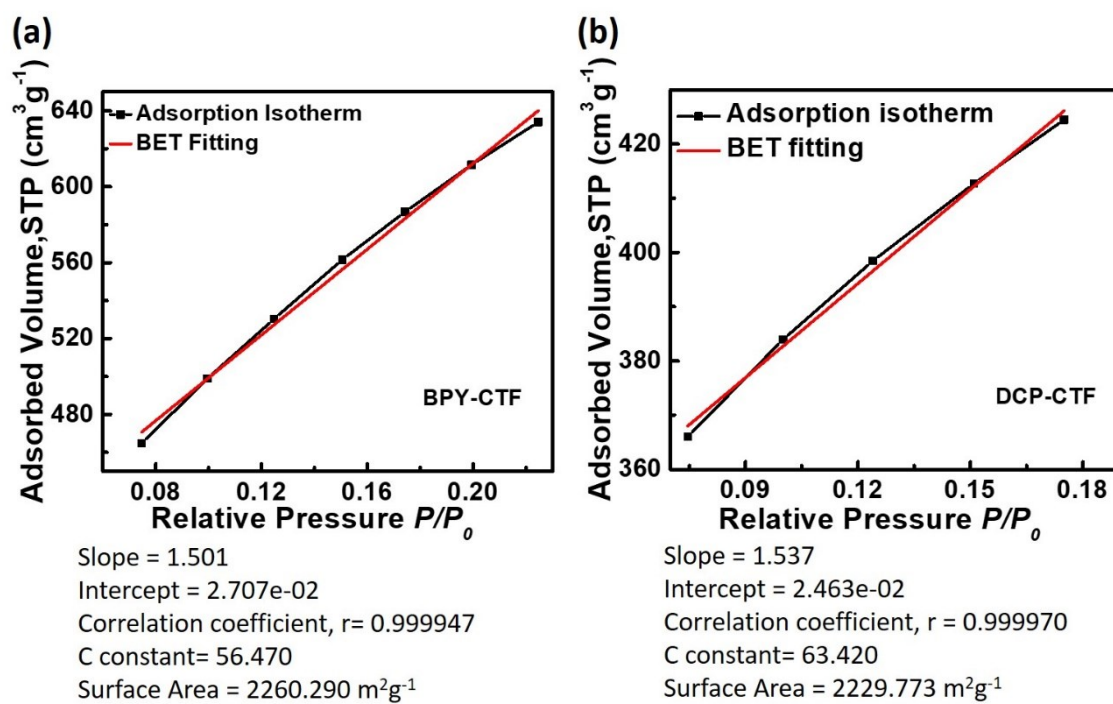


Fig. S3 The calculated pore parameters of (a) BPY-CTF and (b) DCP-CTF.

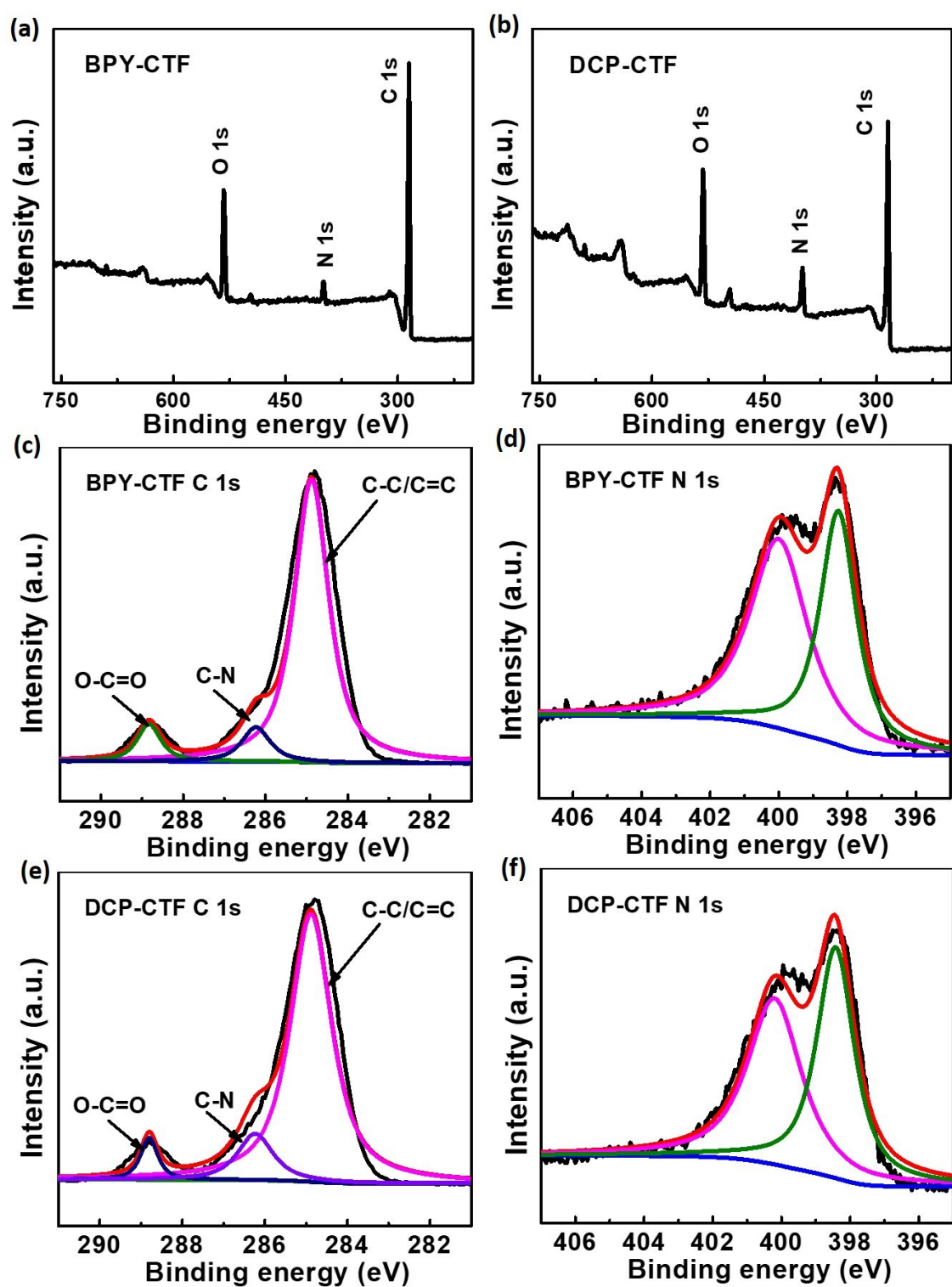


Fig. S4 The XPS spectra of (a) BPY-CTF and (b) DCP-CTF. The deconvoluted (c) C 1s and (d) N 1s of BPY-CTF. The deconvoluted (e) C 1s and (f) N 1s of DCP-CTF.

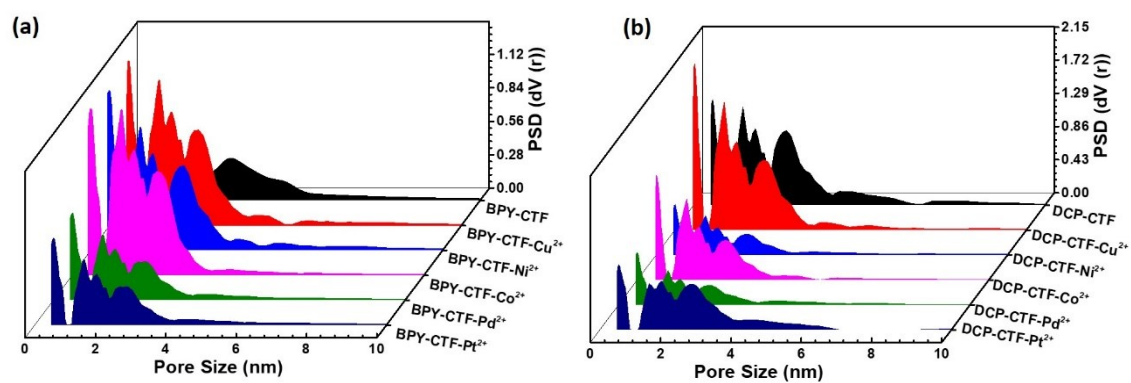


Fig. S5 The pore size distribution profiles calculated by QS-DTF for (a) BPY-CTF-M²⁺ and (b) DCP-CTF-M²⁺.

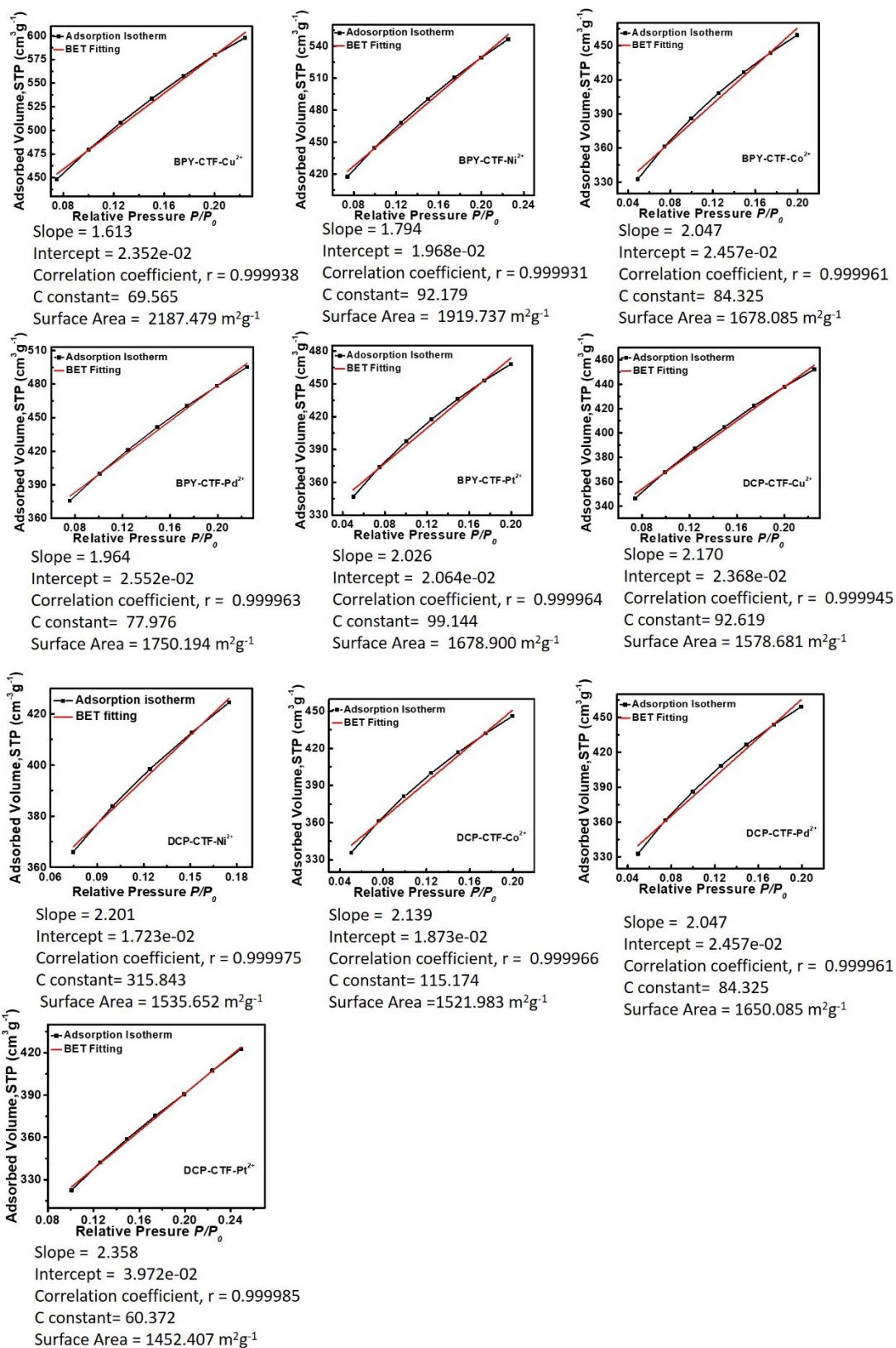


Fig. S6 The calculated pore parameters of BPY-CTF-M²⁺ and DCP-CTF-M²⁺.

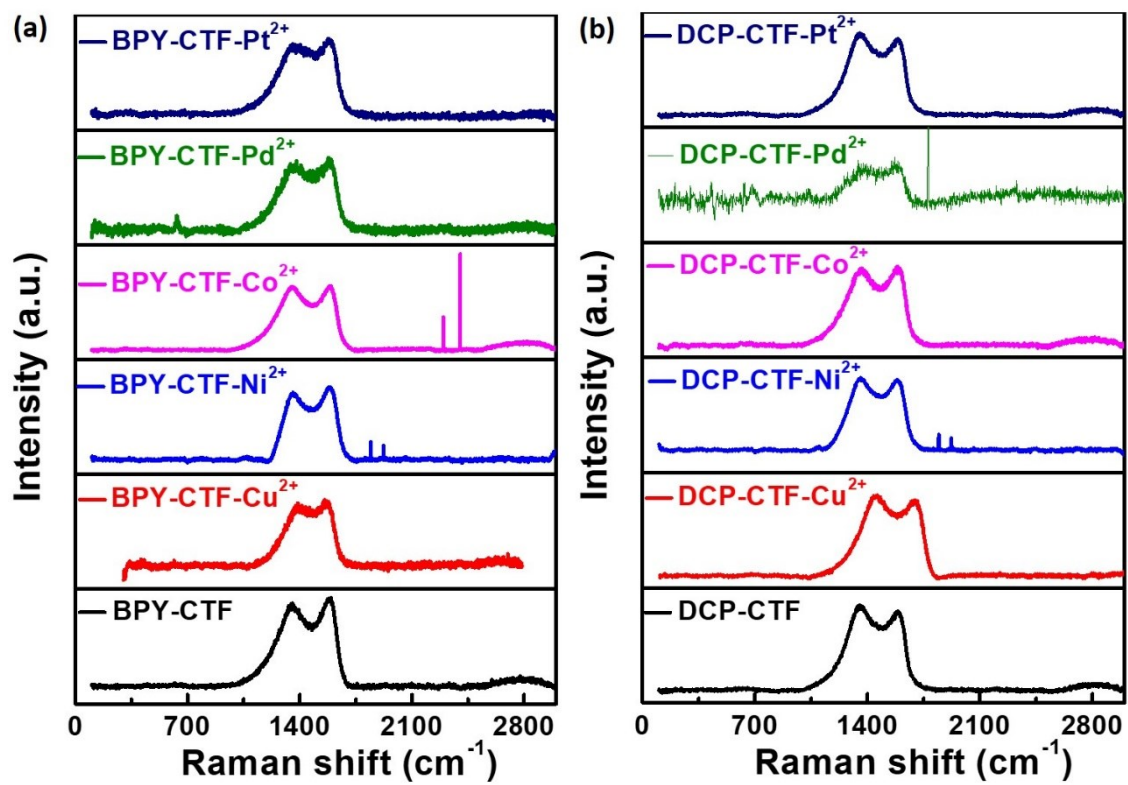


Fig. S7 Raman spectra of BPY-CTF-M²⁺ and DCP-CTF-M²⁺.

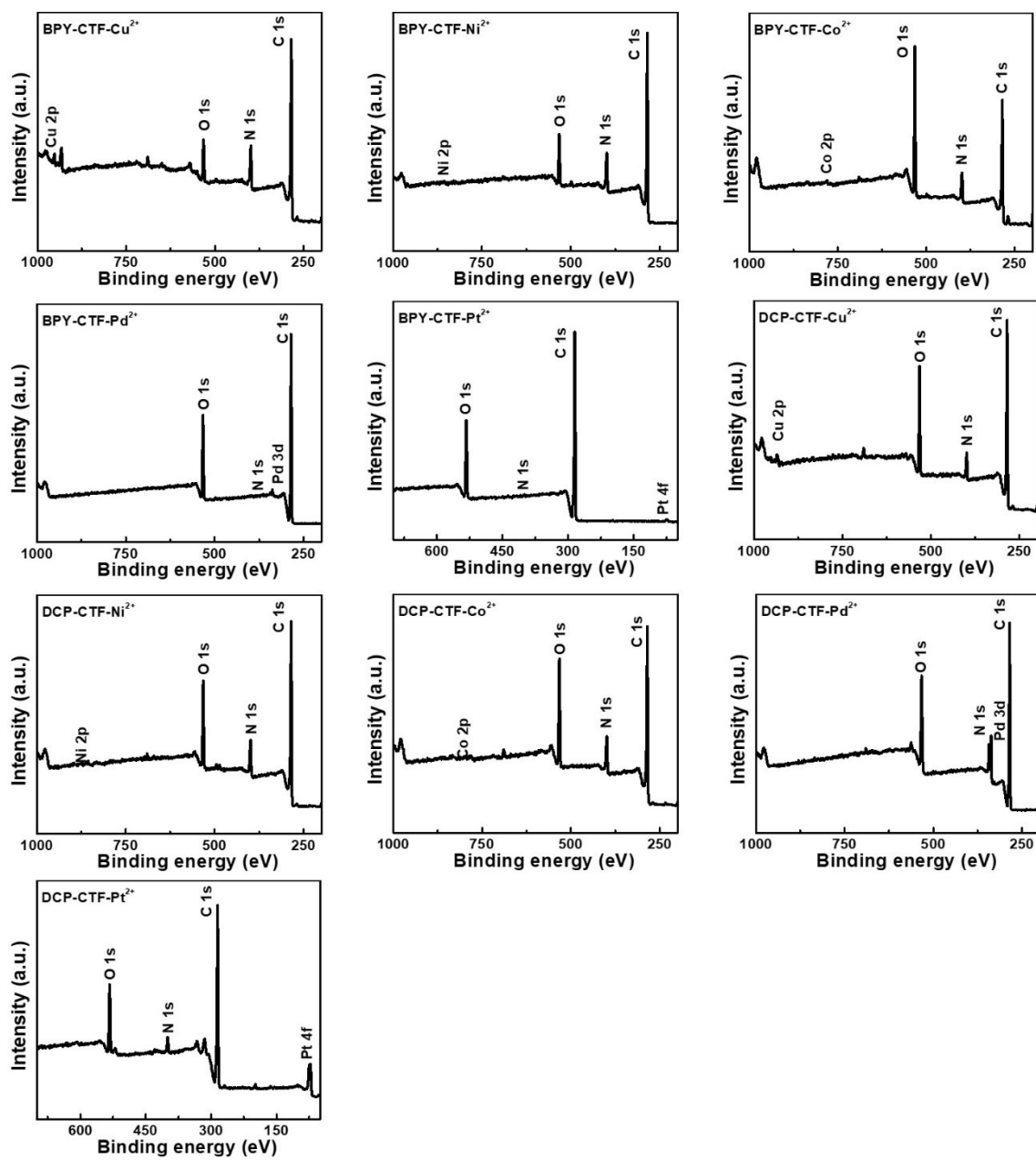


Fig. S8 The XPS spectra of BPY-CTF-M²⁺ and DCP-CTF-M²⁺.

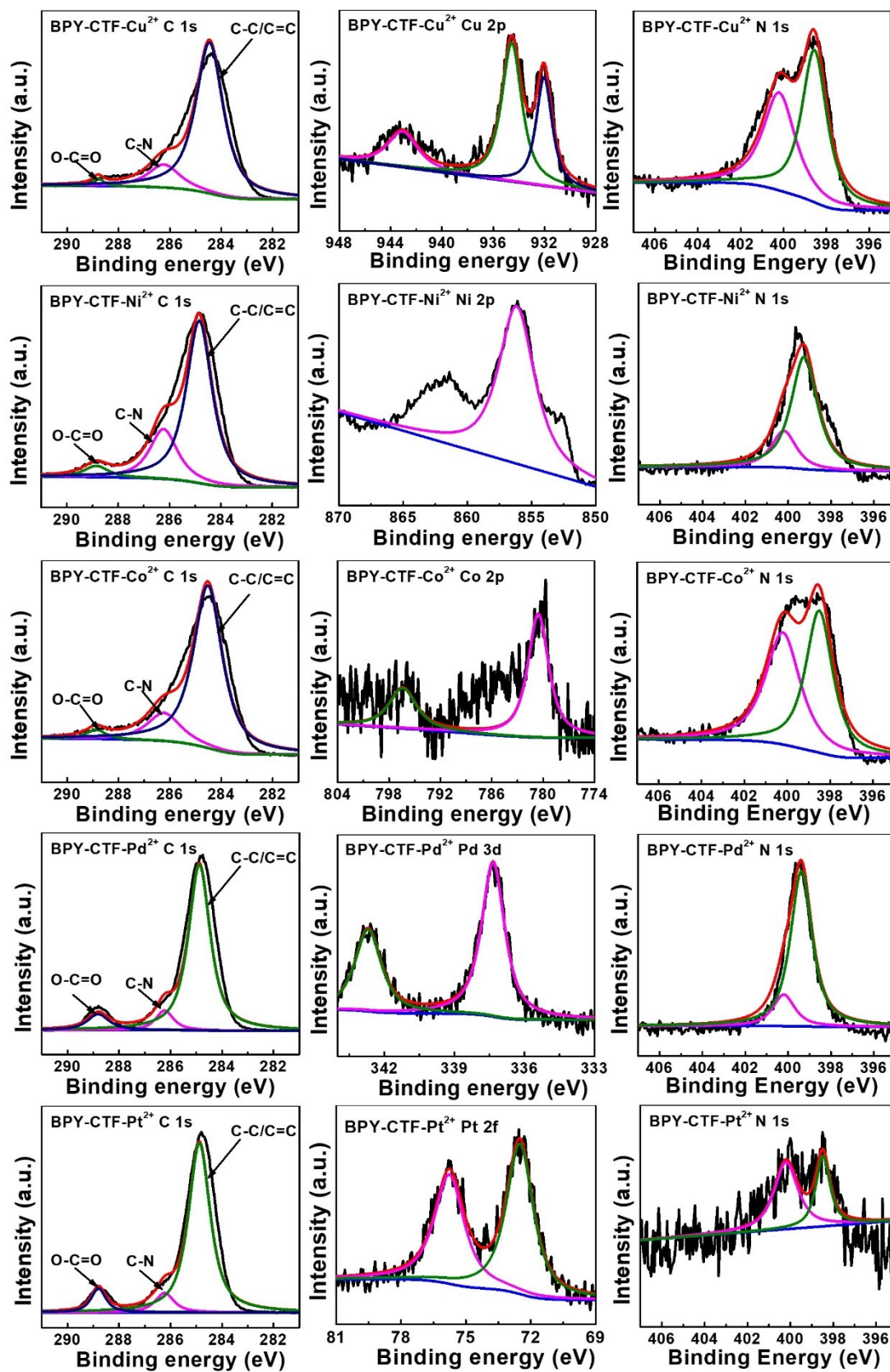


Fig. S9 The deconvoluted C 1s, N 1s, and metal elements for BPY-CTF-M²⁺.

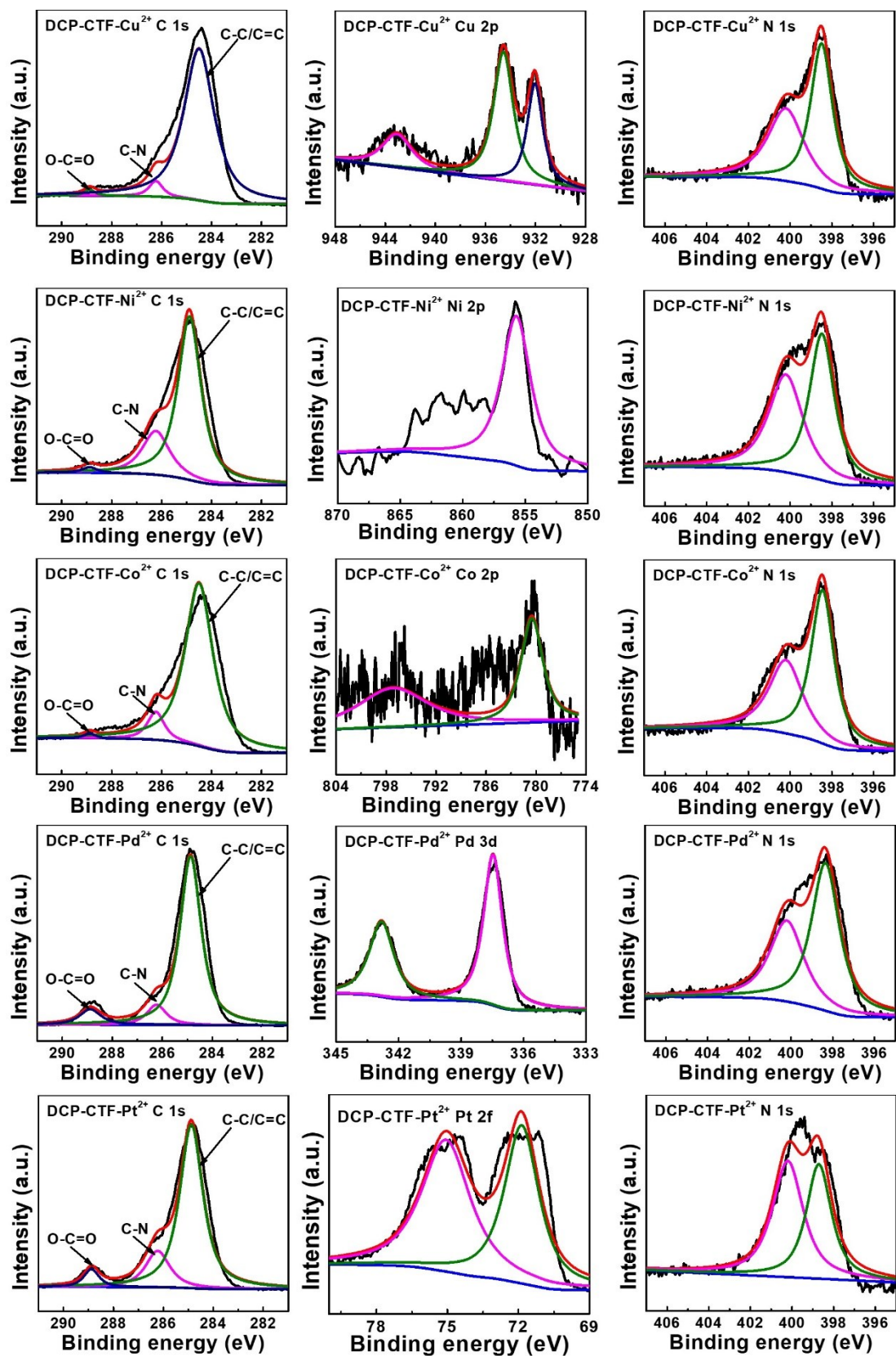


Fig. S10 The deconvoluted C 1s, N 1s, and metal elements for DCP-CTF-M²⁺.

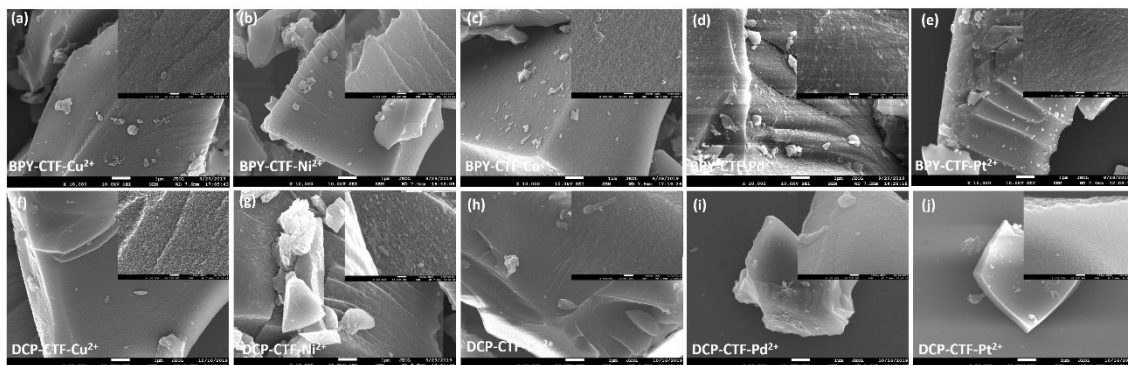


Fig. S11 The SEM images of BPY-CTF- M^{2+} and DCP-CTF- M^{2+} .

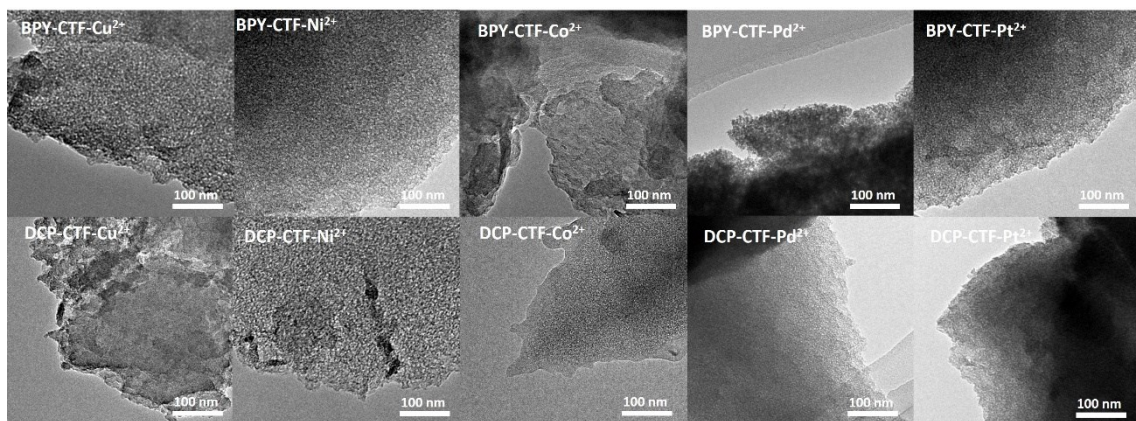


Fig. S12 The TEM images of BPY-CTF- M^{2+} and DCP-CTF- M^{2+} .

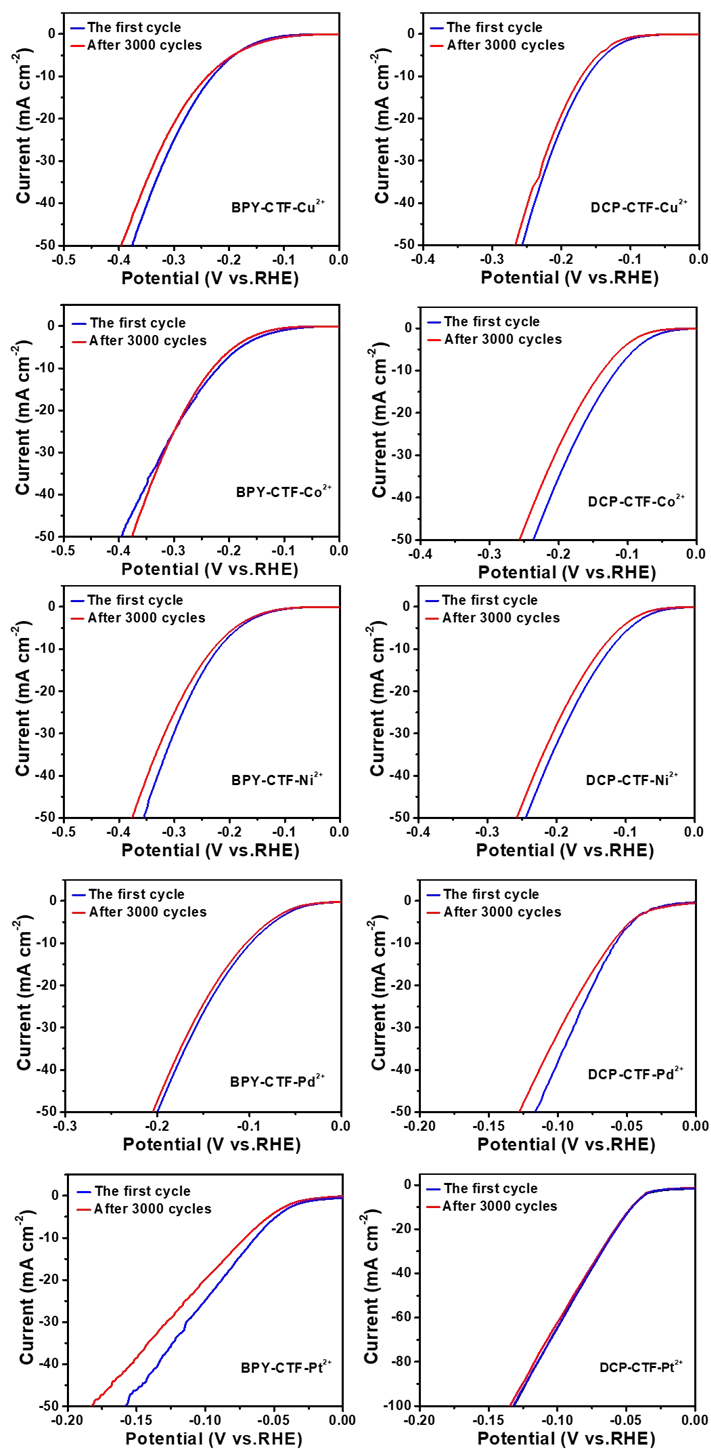


Fig. S13 Cycling stability of CTF-M²⁺ in aqueous H₂SO₄ solution (0.5 mol L⁻¹).

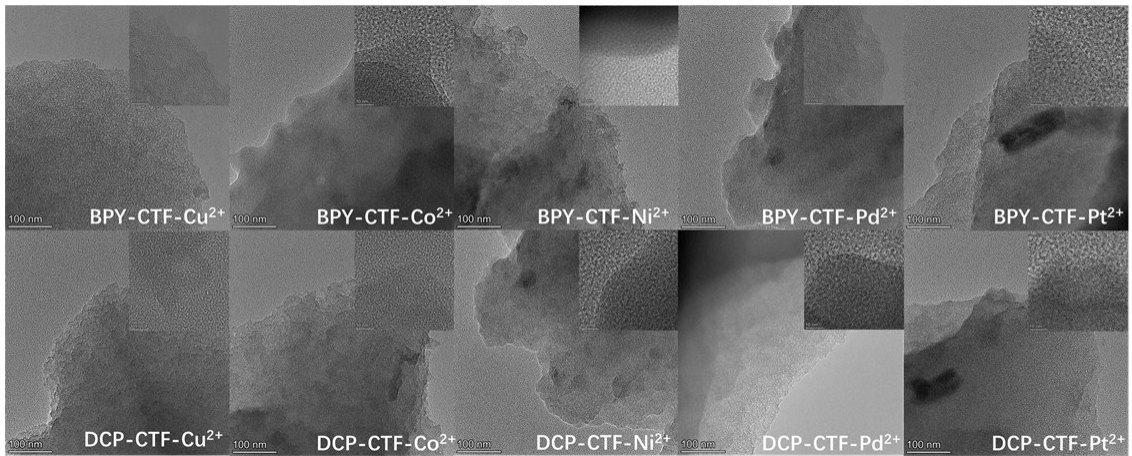


Fig. S14 TEM images of CTF- M^{2+} after 3000 cycles were tested by CV measurement.

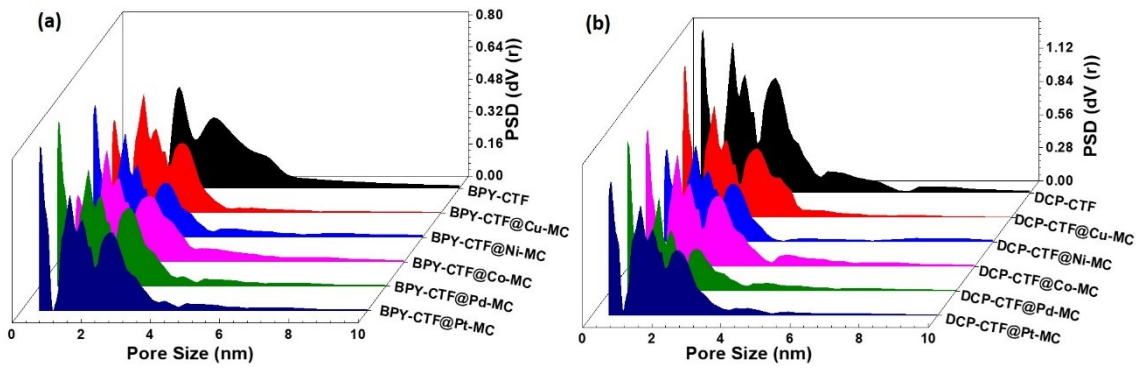
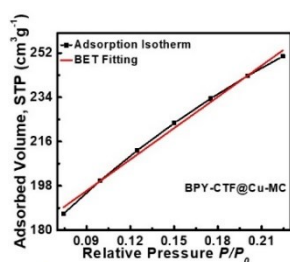
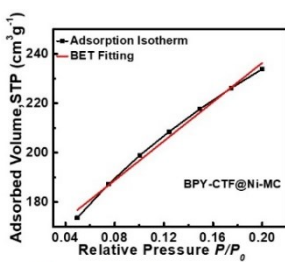


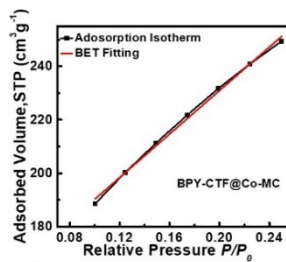
Fig. S15 The pore size distribution profiles calculated by QS-DTF for (a) BPY-CTF@MC and (b) DCP-CTF@MC.



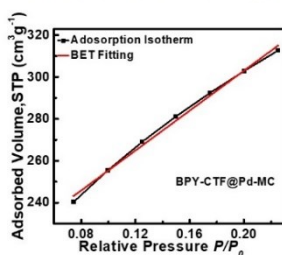
Slope = 3.840
 Intercept = 5.788e-02
 Correlation coefficient, $r = 0.999933$
 C constant= 67.347
 Surface Area = 893.375 m^2g^{-1}



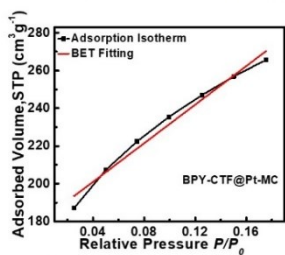
Slope = 4.067
 Intercept = 3.973e-02
 Correlation coefficient, $r = 0.999975$
 C constant= 103.360
 Surface Area = 848.001 m^2g^{-1}



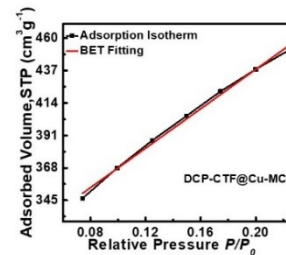
Slope = 3.962
 Intercept = 7.342e-02
 Correlation coefficient, $r = 0.999895$
 C constant= 54.968
 Surface Area = 862.942 m^2g^{-1}



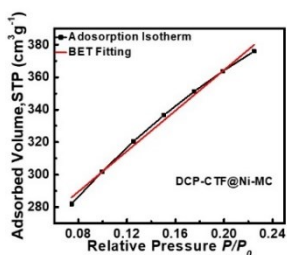
Slope = 3.146
 Intercept = 3.205e-02
 Correlation coefficient, $r = 0.999935$
 C constant= 99.159
 Surface Area = 1095.705 m^2g^{-1}



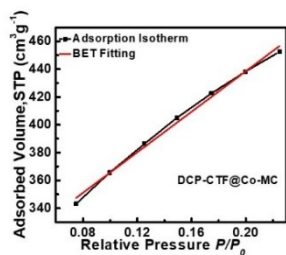
Slope = 3.504
 Intercept = 2.582e-02
 Correlation coefficient, $r = 0.999934$
 C constant= 136.716
 Surface Area = 986.480 m^2g^{-1}



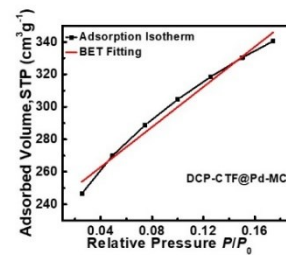
Slope = 2.170
 Intercept = 2.368e-02
 Correlation coefficient, $r = 0.999945$
 C constant= 92.619
 Surface Area = 1537.681 m^2g^{-1}



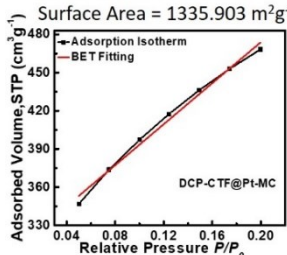
Slope = 2.571
 Intercept = 3.591e-02
 Correlation coefficient, $r = 0.999907$
 C constant= 72.599
 Surface Area = 1335.903 m^2g^{-1}



Slope = 2.21
 Intercept = 1.033e-02
 Correlation coefficient, $r = 0.999975$
 C constant= 215.843
 Surface Area = 1556.752 cm^2g^{-1}



Slope = 2.746
 Intercept = 1.682e-02
 Correlation coefficient, $r = 0.999956$
 C constant= 164.293
 Surface Area = 1260.364 m^2g^{-1}



Slope = 2.026
 Intercept = 2.064e-02
 Correlation coefficient, $r = 0.999964$
 C constant= 99.144
 Surface Area = 1701.900 m^2g^{-1}

Fig. S16 The calculated pore parameters of BPY-CTF@MC and DCP-CTF@MC.

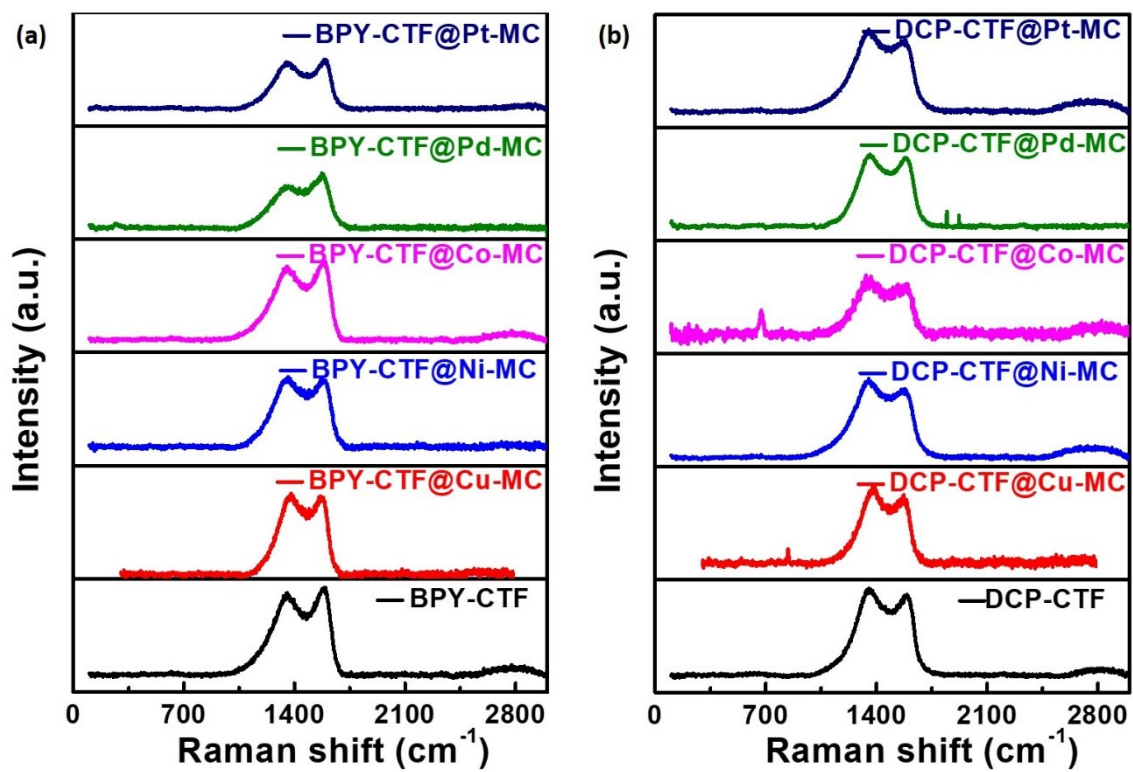


Fig. S17 Raman spectra of BPY-CTF@MC and DCP-CTF@MC.

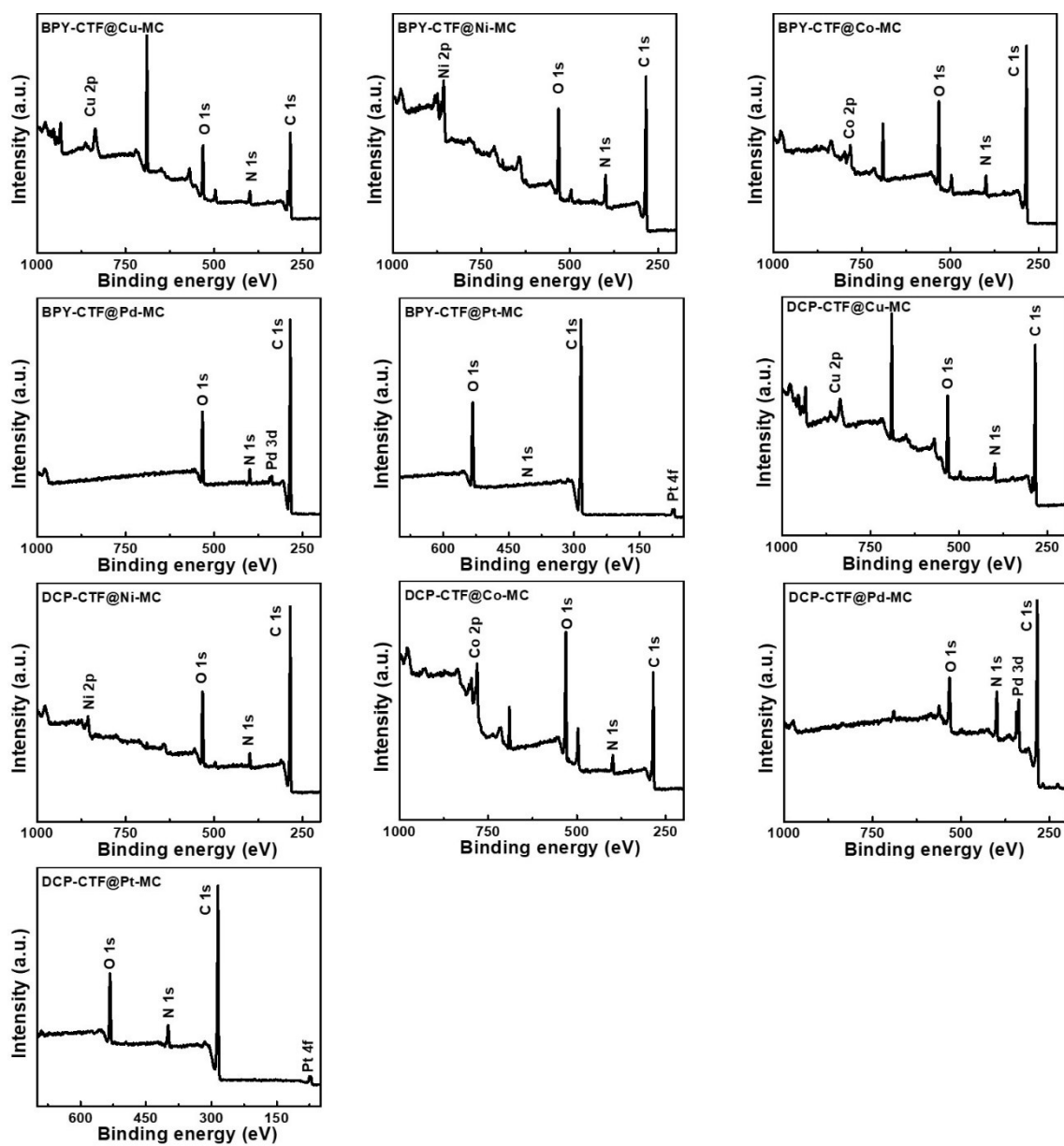


Fig. S18 The XPS spectra of BPY-CTF@MC and (b) DCP-CTF@MC.

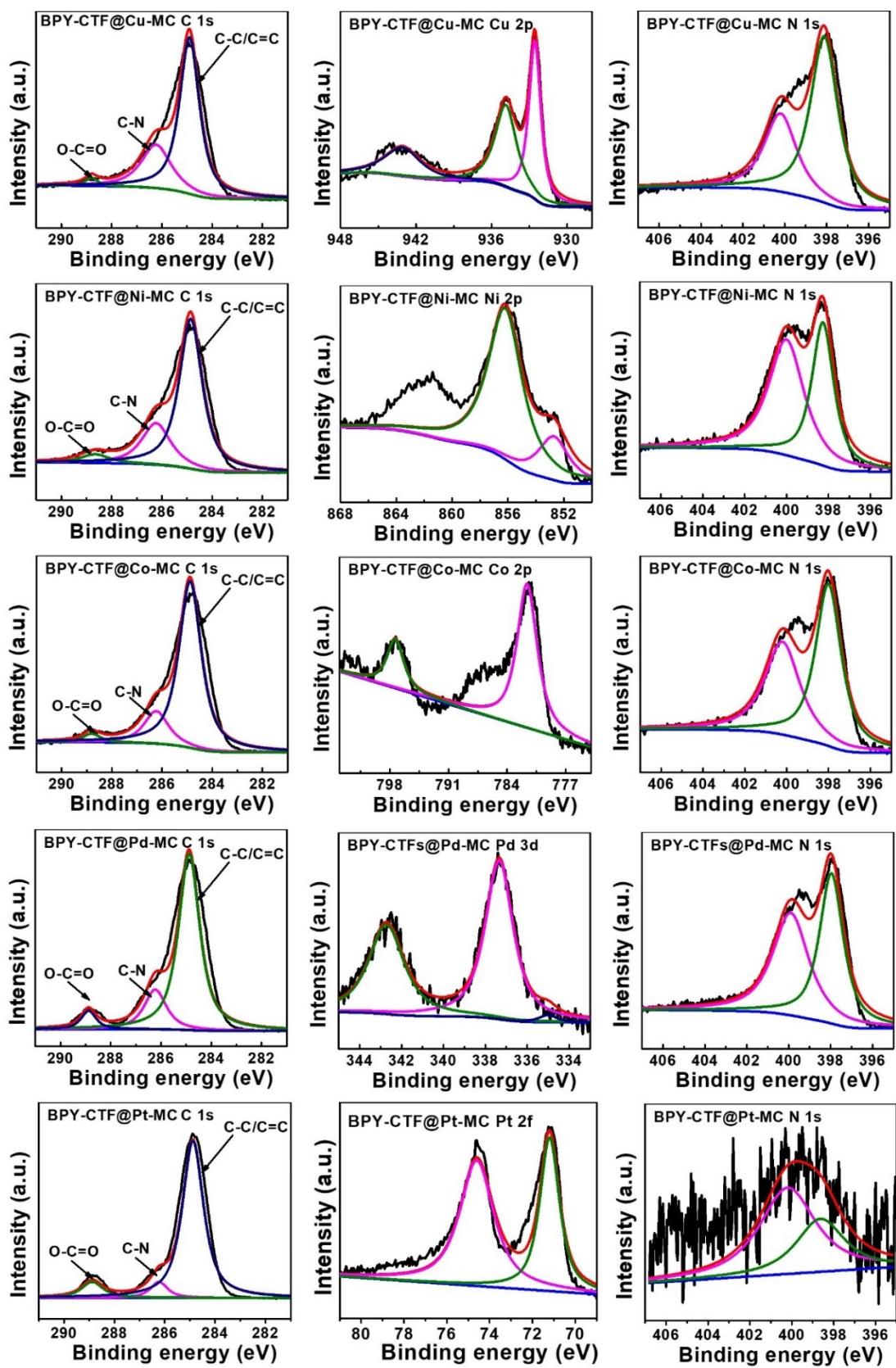


Fig. S19 The deconvoluted C 1s, N1s, and metal element for BPY-CTF@MC.

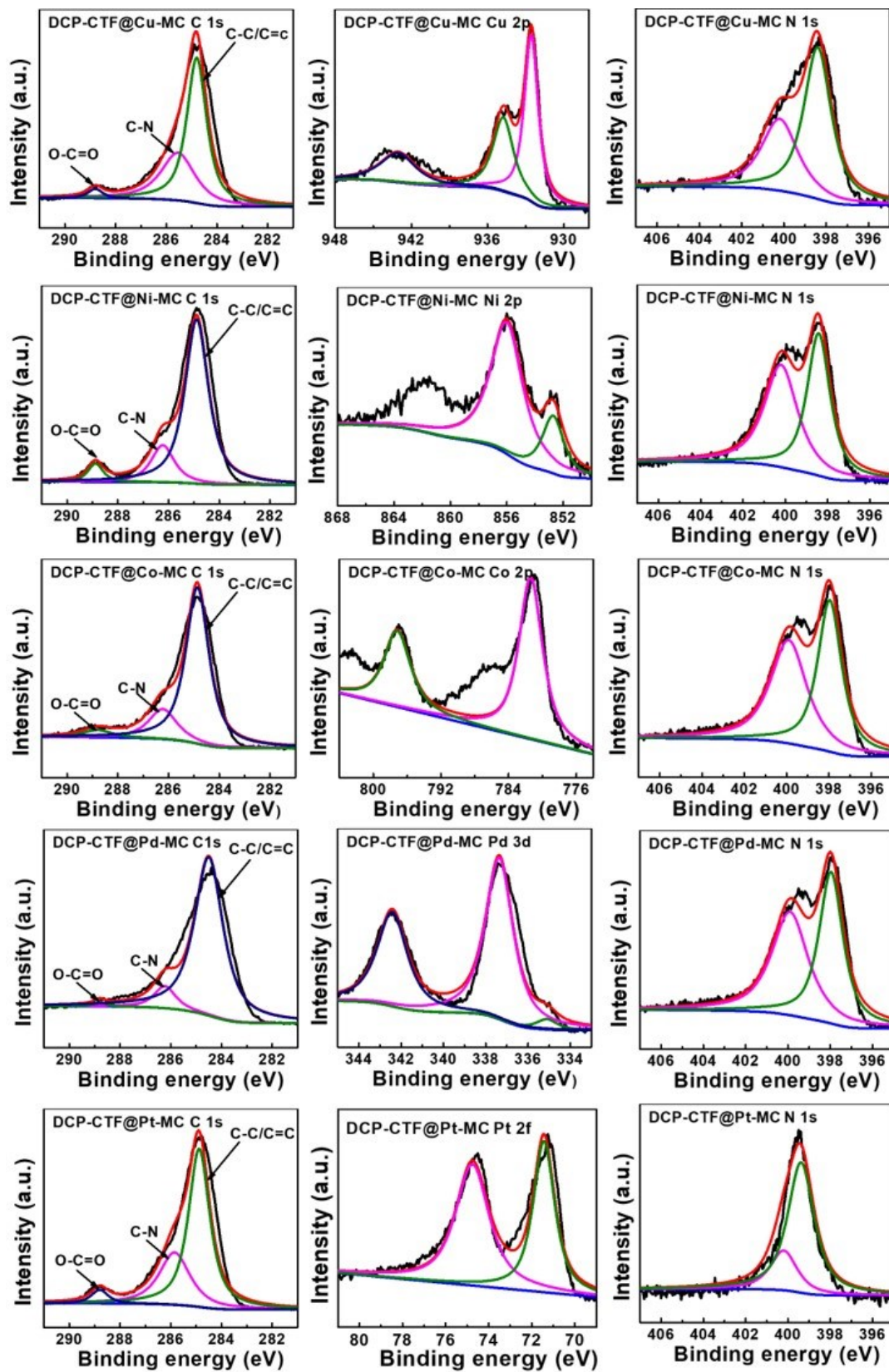


Fig. S20 The deconvoluted C 1s, N1s, and metal element for DCP-CTF@MC.

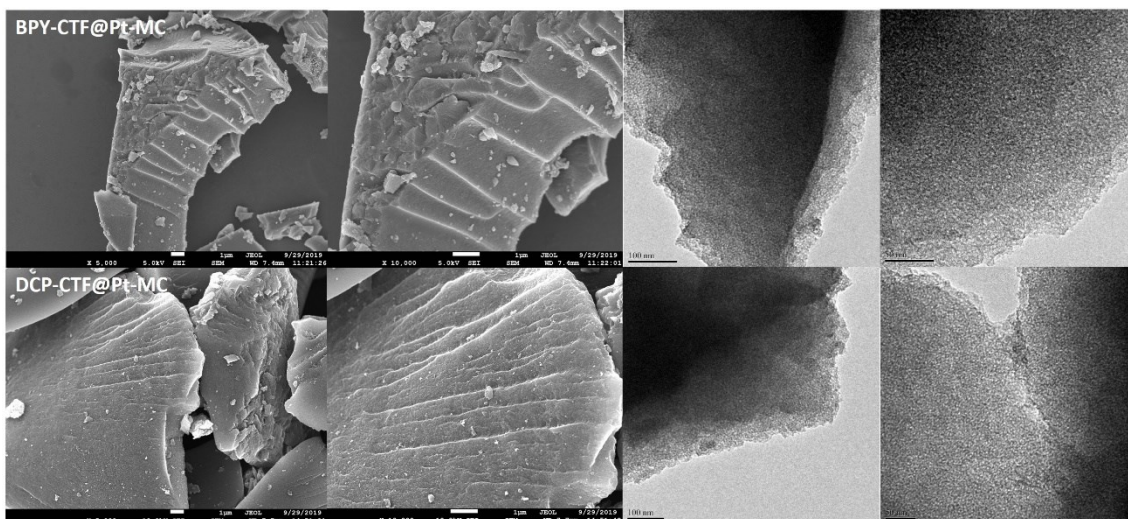


Fig. S21 The SEM and TEM images of BPY-CTF@Pt-MC and DCP-CTF@Pt-MC.

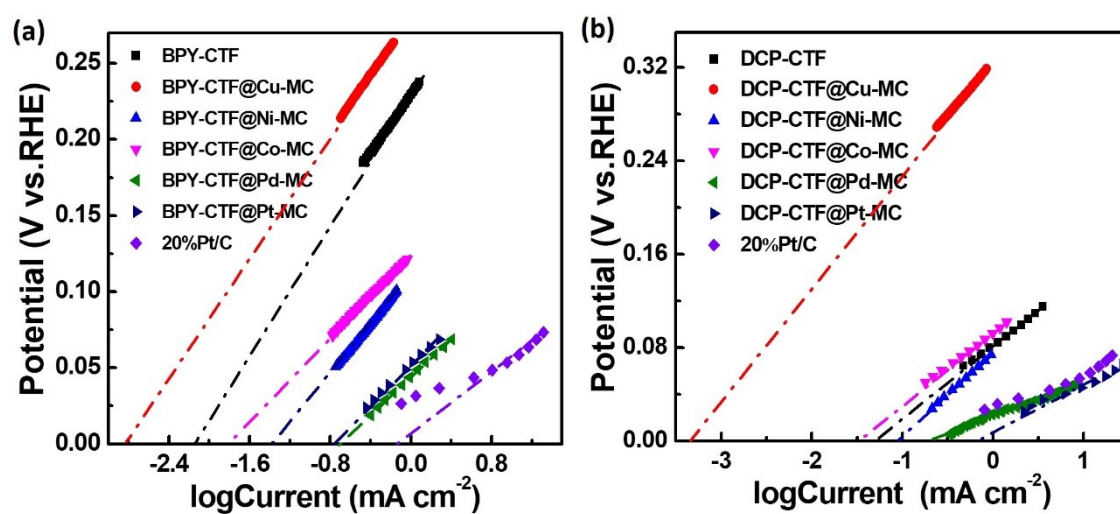


Fig. S22 Exchange current density (i_0) of commercial 20 % Pt/C, BPY-CTF@MC, and DCP-CTF@MC using extrapolation method.

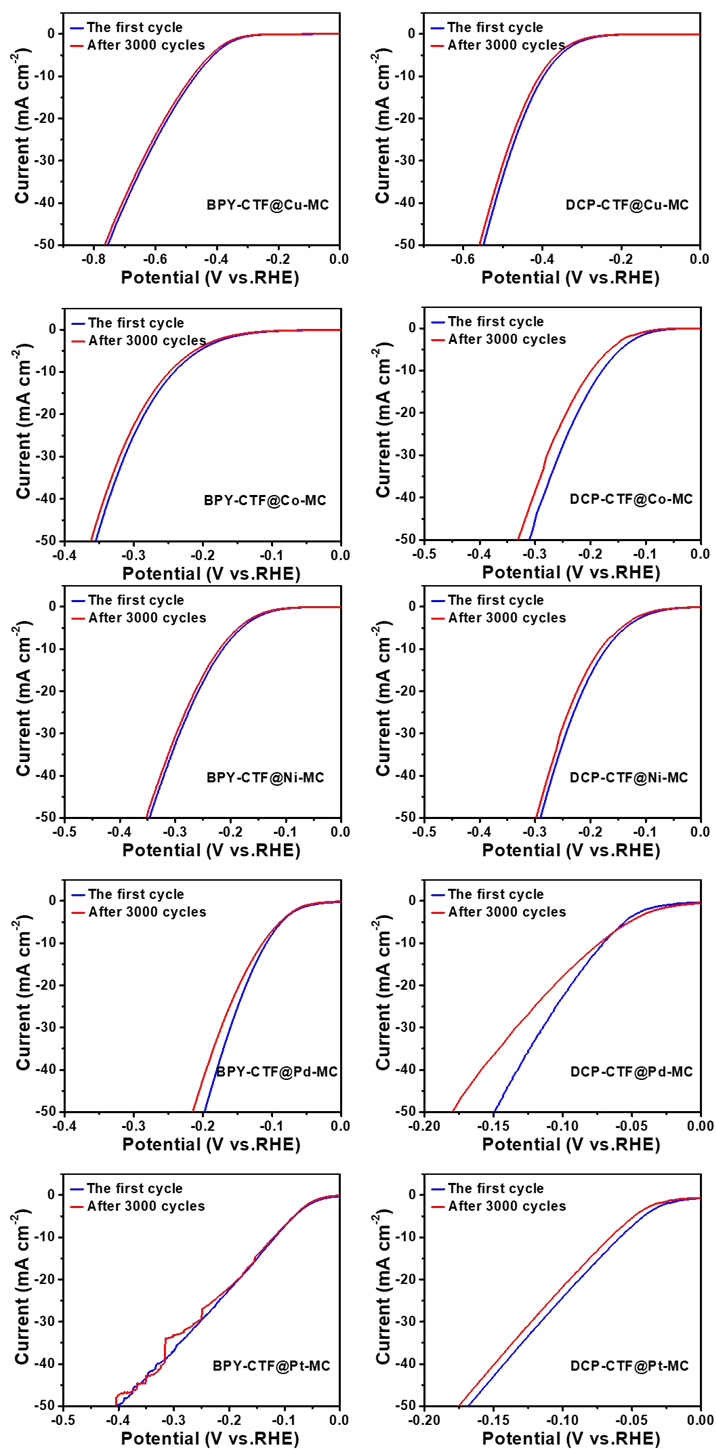


Fig. S23 Cycling stability of CTF@MC in aqueous H_2SO_4 solution (0.5 mol L^{-1}).

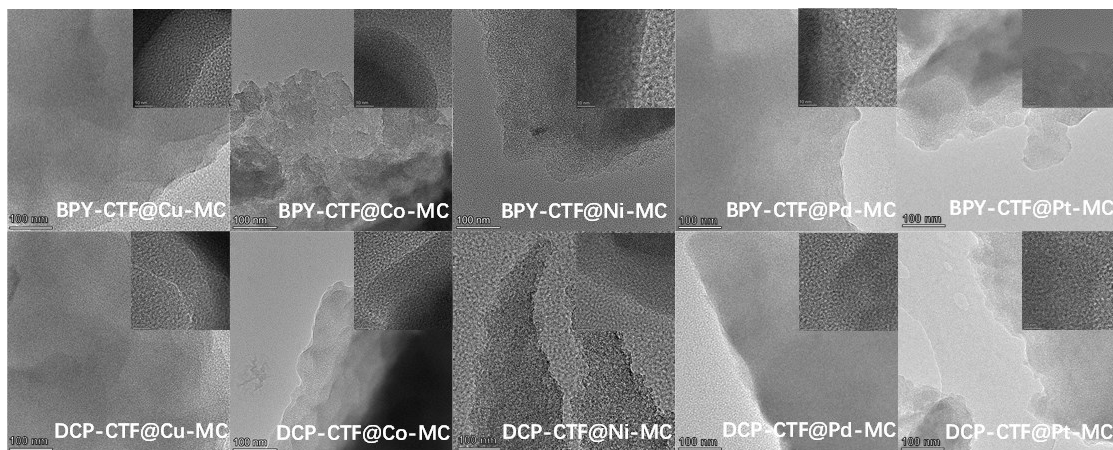


Fig. S24 TEM images of CTF@MC after 3000 cycles were tested by CV measurement.

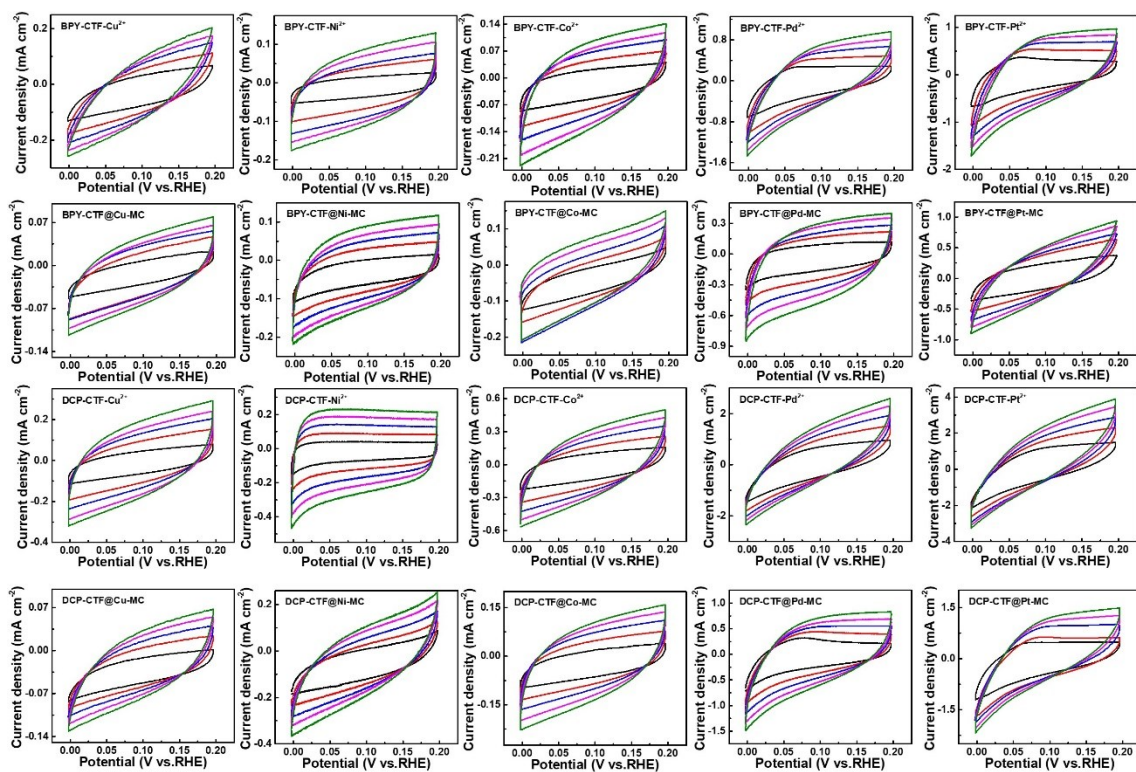


Fig. S25 Cyclic voltammety curves of CTF-M²⁺ and CTF@MC in the region of 0.00–0.20 V vs. RHE.

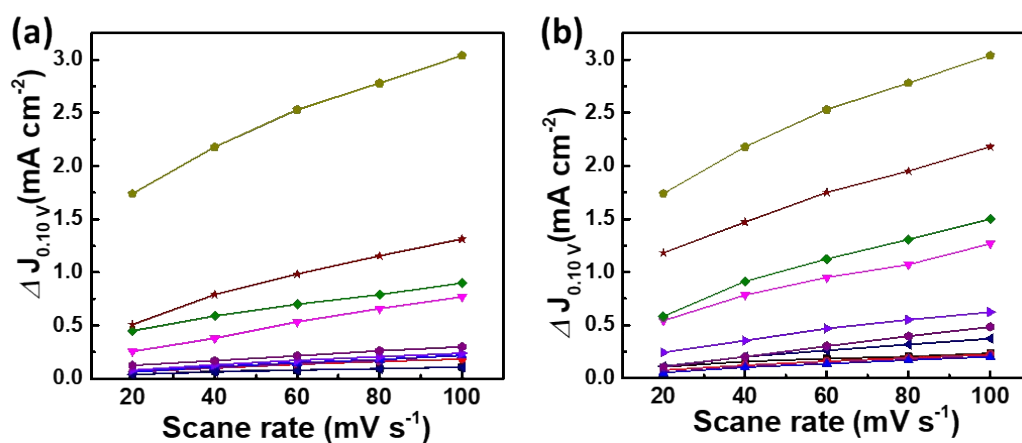


Fig. S26 The capacitive current densities at 0.1 V as a function of scan rate for (a) CTF- M^{2+} (black: BPY-CTF-Cu $^{2+}$; red: BPY-CTF-Co $^{2+}$; blue: BPY-CTF-Ni $^{2+}$; pink: BPY-CTF-Pd $^{2+}$; green: BPY-CTF-Pt $^{2+}$; mazarine: DCP-CTF-Cu $^{2+}$; violet: DCP-CTF-Co $^{2+}$; purple: DCP-CTF-Ni $^{2+}$; wine: DCP-CTF-Pd $^{2+}$; dark yellow: DCP-CTF-Pt $^{2+}$) and (b) CTF@M (black: BPY-CTF@Cu-MC; red: BPY-CTF@Co-MC; blue: BPY-CTF@Ni-MC; pink: BPY-CTF@Pd-MC; green: BPY-CTF@Pt-MC; mazarine: DCP-CTF@Cu-MC; violet: DCP-CTF@Co-MC; purple: DCP-CTF@Ni-MC; wine: DCP-CTF@Pd-MC; dark yellow: DCP-CTF@Pt-MC).

Theoretical Calculations

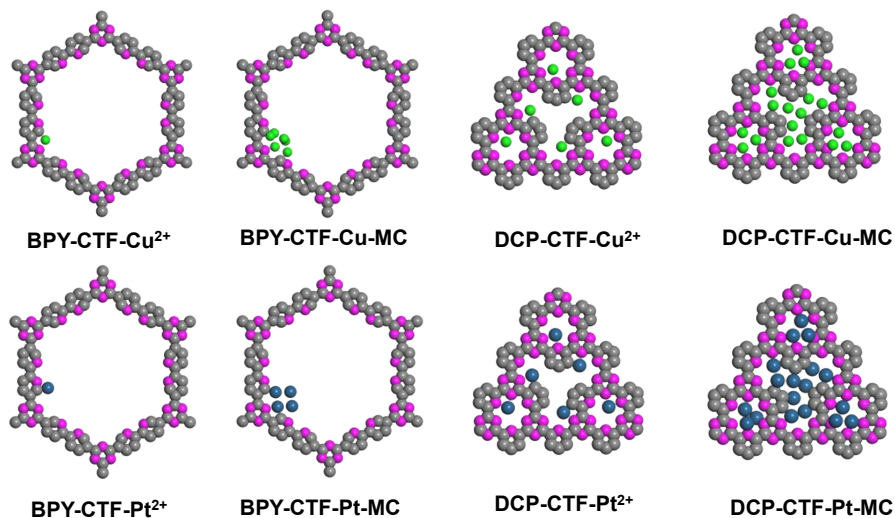


Fig. S27 Structure models for CTF-Cu²⁺, CTF-Cu-MC, CTF-Pt²⁺, and CTF-Pt-MC.

Grey, pink, green and blue sphere are corresponding to C, N, Cu, and Pt atoms, respectively.

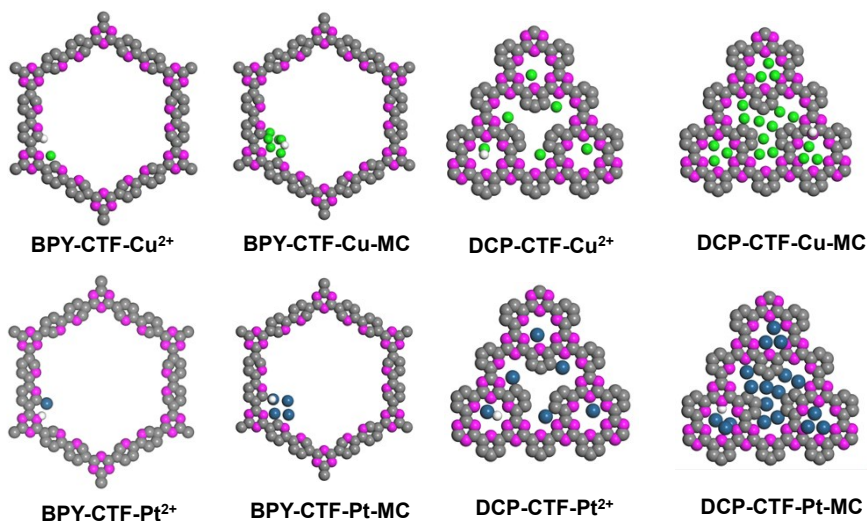
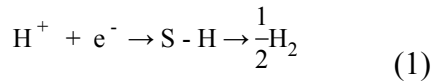


Fig. S28 Structure models of hydrogen adsorption for CTF-Cu²⁺, CTF-Cu-MC, CTF-

Pt²⁺, and CTF-Pt-MC. Grey, pink, green, blue and white sphere are corresponding to C, N, Cu, Pt, and H atoms, respectively.

The projector-augmented wave pseudopotential^{S2} and the Perdew–Burke–Ernzerhof (PBE) exchange-correlation function with a 450 eV plane-wave cutoff energy were applied during the calculation. The atomic positions, cell shape, and cell volume were fully optimized until the force on each atom was less than 0.05 eV. The Structure models and structure models of hydrogen adsorption for CTF-Cu²⁺, CTF-Cu-MC, CTF-Pt²⁺, and CTF-Pt-MC have been shown in Fig. S27 and S28.

The global reaction pathway can be represented as a three state mechanism.



where S represents an adsorption site on the considered surface model.

The computation of ΔG_{H} is accomplished within its general definition related to the first reaction step in Eq.(1):

$$\Delta G_{\text{H}} = \Delta E_{\text{H}} + \Delta E_{\text{ZPE}} - T\Delta S \quad (2)$$

Here ΔE_{H} is the H-adsorption energy, ΔE_{ZPE} is the variation of the zero point energy along the first step implicated in Eq.(1) and $T\Delta S$ represents the entropic barrier related with the entropy losses due to the adsorption of the hydrogen atom.

The H-adsorption energy ΔE_{H} is defined as:

$$\Delta E_{\text{H}} = \frac{1}{n}[E_{(\text{S} + n\text{H})} - E_{(\text{S})} - \frac{n}{2}E_{(\text{H}_2)}] \quad (3)$$

Where n is the number of hydrogen atoms adsorbed on the surface S, and E is the DFT energy.

Table S1. Elemental analyses of BPY-CTF and DCP-CTF by XPS.

	C 1s		N 1s		O 1s	
	<i>Atomic %</i>	<i>wt %</i>	<i>Atomic %</i>	<i>wt %</i>	<i>Atomic %</i>	<i>wt %</i>
BPY-CTF	67.17	61.52	10.48	11.20	22.35	27.27
DCP-CTF	78.31	74.44	12.12	13.44	9.57	12.11

The composition ratios (*atomic %*) for BPY-CTF and DCP-CTF estimated from the XPS results.

Take the calculation of N content as an example:

$$N(\text{wt \%}) = \frac{N(\text{Atomic \%}) * 14.01}{C(\text{Atomic \%}) * 12.01 + N(\text{Atomic \%}) * 14.01 + O(\text{Atomic \%}) * 16.00}$$

Table S2. Comparison of specific surface areas of BPY-CTF, DCP-CTF, BPY-CTF-M²⁺, DCP-CTF-M²⁺, BPY-CTF@MC, and DCP-CTF@MC.

Catalyst	BET Specific Surface Area (m ² g ⁻¹)
BPY-CTF	2260
BPY-CTF-Cu ²⁺	2180
BPY-CTF-Co ²⁺	1560
BPY-CTF-Ni ²⁺	1920
BPY-CTF-Pd ²⁺	1750
BPY-CTF-Pt ²⁺	1680
BPY-CTF@Cu-MC	890
BPY-CTF@Co-MC	860
BPY-CTF@Ni-MC	850
BPY-CTF@Pd-MC	990
BPY-CTF@Pt-MC	1100
DCP-CTF	2230
DCP-CTF-Cu ²⁺	1580
DCP-CTF-Co ²⁺	1520
DCP-CTF-Ni ²⁺	1540
DCP-CTF-Pd ²⁺	1670
DCP-CTF-Pt ²⁺	1460
DCP-CTF@Cu-MC	1540
DCP-CTF@Co-MC	1560
DCP-CTF@Ni-MC	1340
DCP-CTF@Pd-MC	1260
DCP-CTF@Pt-MC	1700

Table S3. Comparison of electrocatalytic properties of BPY-CTF, DCP-CTF, BPY-CTF-M²⁺, DCP-CTF-M²⁺, BPY-CTF@MC, and DCP-CTF@MC.

Catalyst	Overpotential/mV @10mA cm ⁻² versus RHE	Tafel slope (mV dec ⁻¹)	Exchange current density (mA cm ⁻²)	C _{dl} (mF cm ⁻²)
BPY-CTF	345	94.3	0.0055	1.50
BPY-CTF-Cu ²⁺	230	77.4	0.0120	1.52
BPY-CTF-Co ²⁺	221	66.2	0.0320	1.82
BPY-CTF-Ni ²⁺	220	66.8	0.0370	1.83
BPY-CTF-Pd ²⁺	99	51.5	0.0690	8.68
BPY-CTF-Pt ²⁺	66	47.1	0.3300	11.10
BPY-CTF@Cu-MC	470	95.6	0.0020	0.08
BPY-CTF@Co-MC	234	82.0	0.0160	1.51
BPY-CTF@Ni-MC	213	80.7	0.0430	1.93
BPY-CTF@Pd-MC	109	61.9	0.1900	6.54
BPY-CTF@Pt-MC	117	62.0	0.1700	6.20
DCP-CTF	155	53.4	0.0340	3.77
DCP-CTF-Cu ²⁺	162	55.3	0.0140	3.20
DCP-CTF-Co ²⁺	121	44.3	0.0620	4.77
DCP-CTF-Ni ²⁺	121	45.0	0.0780	4.80
DCP-CTF-Pd ²⁺	58	38.2	0.1720	12.40
DCP-CTF-Pt ²⁺	46	30.2	0.4100	16.00
DCP-CTF@Cu-MC	397	90.2	0.0050	0.80
DCP-CTF@Co-MC	181	57.4	0.0400	1.98
DCP-CTF@Ni-MC	176	55.6	0.1000	2.20
DCP-CTF@Pd-MC	71	45.6	0.2200	9.60
DCP-CTF@Pt-MC	60	30.7	0.4000	12.05

References

- [S1] S. Hug, L. Stegbauer, H. Oh, M. Hirscher and B. V. Lotsch, Nitrogen-rich covalent triazine frameworks as high-performance platforms for selective carbon capture and storage. *Chem. Mater.* **2015**, *27* (23), 8001–8010. [DOI: 10.1021/acs.chemmater.5b03330](https://doi.org/10.1021/acs.chemmater.5b03330)
- [S2] J. P. Perdew, J. A. Chevary, S. H. Vosko, K. A. Jackson, M. R. Pederson, D. J. Singh and C. Fiolhais, Atoms, molecules, solids, and surfaces: applications of the generalized gradient approximation for exchange and correlation, *Phys. Rev. B*, 1992, **46** (11), 06671–6687. [DOI: 10.1103/PhysRevB.48.4978.2](https://doi.org/10.1103/PhysRevB.48.4978.2)